The embedded-atom model applied to vacancy formation in bulk aluminium and lithium

1999 J. Phys.: Condens. Matter 11 3663

(http://iopscience.iop.org/0953-8984/11/18/303)

J. Phys.: Condens. Matter **11** (1999) 3663–3677. Printed in the UK PII: S0953-8984(99)01684-7

The embedded-atom model applied to vacancy formation in bulk aluminium and lithium

P M Derlet†, R Høier†, R Holmestad†, K Marthinsen‡ and N Ryum‡

† Department of Physics, Norwegian University of Science and Technology (NTNU), N-7034 Trondheim, Norway

‡ Department of Metallurgy, Norwegian University of Science and Technology (NTNU), N-7034 Trondheim, Norway

Received 9 February 1999

Abstract. The embedded-atom model (EAM) is applied to the study of vacancy formation in bulk aluminium and lithium. A systematic study is undertaken into the sensitivity of the EAM potentials and embedding energy functionals as a function of the unrelaxed vacancy formation energy which is normally obtained via *ab initio* density functional calculations. The effect of this 'empirical' input parameter on the vacancy relaxation energy, formation volume and structural relaxation is also investigated using super-cell sizes not normally accessible in orbital-based *ab initio* relaxation studies. We find that for aluminium, for which at most a fifth-nearest-neighbour model is required, the vacancy relaxation energy and formation volume are not sensitive functions of the unrelaxed vacancy formation energy. For lithium, for which at least a ninth-nearest-neighbour model is needed, the situation is somewhat different: both the vacancy relaxation energy and the formation volume are found to be a noticeably related to the unrelaxed vacancy formation energy. For both solids, the structural relaxation was found to be largely insensitive to the unrelaxed vacancy formation energy, agreeing well with previous *ab initio* calculations. In particular for aluminium, the EAM result agrees extremely well with recent orbital-free density functional calculations which use super-cell sizes approaching those used here. Finally, we find that for lithium, the embedding energy functional has negligible curvature for a wide range of local electronic densities, justifying the use of a simpler pair potential description for lithium in mildly inhomogeneous systems.

1. Introduction

With the advent of density functional molecular dynamics [1, 2], the simulation of relatively large super-cells in which both the ionic and electronic degrees of freedom are treated in an *ab initio* way provides a powerful first-principles tools for studying the properties of complex materials. The underlying disadvantage is that for metals the orbital-based procedure typically scales as N^3 (where in this case N is the number of atoms per super-cell) and therefore cannot be currently applied to systems beyond a few hundred atoms. On the other hand, orbital-free density functional theory [3–5] (DFT) shows promising signs of achieving near order-N scalability, although the correct choice of the kinetic energy functional is still somewhat arbitrary and for many materials (such as lithium) an adequate local pseudopotential description does not yet exist.

To study alloy systems, large super-cell molecular-dynamics (MD) simulations are needed and a less fundamental calculation of the cohesive energy is therefore needed. The embedded-atom model [6, 7] (EAM) provides one such description, providing a physically appealing picture of the interactions between atoms (ions) that is especially suited to metals—where the

0953-8984/99/183663+15$19.50

electronic contribution to the cohesive energy dominates. Here, for each single-atom energy contribution, there exists, in addition to an (effective) electrostatic inter-atomic potential, an energy term depending on the local electronic density and thereby replacing the global density-dependent term often arising when considering the nearly-free-electron gas of metals. This term is referred to as the embedding energy and represents the energy required to place an atom in its surrounding unperturbed electron density. With such a local definition of volume through the local electron density, the EAM is particularly suited to the study of inhomogeneous systems and has been applied to a variety of large systems containing up to 10^8 atoms [8].

Although the EAM formalism has its origins in density functional theory, its application is largely semi-empirical. Generally the embedding energy and inter-atomic potentials for a pure substance are chosen to reproduce bulk equilibrium properties. These functions can be formulated to exactly reproduce the bulk equilibrium lattice constant and cohesive energy. The remaining degrees of freedom are determined by numerical fitting to the elastic constants and the unrelaxed vacancy formation energy. The latter is, of course, not experimentally obtainable and one must resort to DFT simulations of super-cells containing a single vacancy. On the other hand, if the relaxation energy (the difference between the relaxed and unrelaxed formation energy) is expected to be small for a particular material, then one may justifiably ignore relaxation effects and use the experimentally obtained relaxed value as a direct input to the EAM fitting procedure.

In the present work we apply the EAM to bulk aluminium and lithium to investigate the corresponding vacancy relaxation processes. Using a range of previously published DFT results for the unrelaxed vacancy formation energy, we examine its effect on the resulting inter-atomic potential and embedding energy functional by calculating the vacancy relaxation energy and measuring the structural relaxation around the vacancy. Although we do not at present consider the composite system, we have chosen aluminium and lithium primarily with a view to developing an EAM representation for the Al–Li family of alloys: commercially important materials for the aerospace industry.

2. The EAM procedure

Within the EAM [6, 7], the total energy of the system is given by the sum of the single-atom energies, E_i, where

$$E_i = F[\rho_i] + \frac{1}{2}\sum_j \phi(r_{ij}) \tag{1}$$

with

$$\rho_i = \sum_j f(r_{ij}). \tag{2}$$

Here $f(r_{ij})$ can be viewed as the electronic density that atom i 'sees' due to atom j and $F[\rho_i]$ as the corresponding embedding energy of atom i when placed in the electronic density arising from the surrounding atoms. $\phi(r_{ij})$ can be interpreted as the effective inter-atomic potential due to electrostatic interaction as well as any modifications that the electronic response may entail.

Equation (1) is invariant with respect to the transformation

$$F[\rho_i] \to F[\rho_i] + \kappa\rho_i \tag{3}$$

$$\phi(r_{ij}) \to \phi(r_{ij}) - 2\kappa f(r_{ij}). \tag{4}$$

This has led Johnson [9] to suggest that for comparison between differing embedding energies and inter-atomic potentials, κ be chosen such that the derivative of $F[\rho_i]$ be zero at the bulk

equilibrium density ρ_e. Thus in the bulk case, the structural contribution to the total energy will be entirely due to the inter-atomic potential. Such a 'standard form' also facilitates a natural representation for the inter-atomic potential between atoms of differing type [9].

Mei *et al* [10, 11] motivated by the work of Johnson [12] developed a method of representation of both the inter-atomic potential and the embedding energy function that can be applied to an arbitrary number of nearest-neighbour shells. This in part has been facilitated by exploiting the universal scaling properties of solids when under compression or tension [13]. Furthermore, a natural form of $f(r_{ij})$ can be obtained from the manner in which the equilibrium electron density scales as a function of nearest-neighbour separation

$$\rho(\bar{r}) = \rho_e \exp\left[-\beta\left(\frac{\bar{r}}{r_e} - 1\right)\right] \tag{5}$$

where r_e (the equilibrium nearest-neighbour distance) and β are specific to the material of interest.

Equation (5) can be equated to a summation over $f(r_{ij})$:

$$\sum_m s_m f(p_m \bar{r}) = \rho(\bar{r}) \tag{6}$$

where s_m is equal to the number of mth-nearest-neighbour atoms at a distance $p_m r_e$. Mei *et al* [10] use a finite Maclaurin series to approximately invert this; however, recently, a multi-dimensional generalization of the Möbius inversion has allowed exact inversion for a variety of crystallographic structures [14]. We employ the latter technique in the present analysis.

By exploiting the universal features of bulk solids (using the cohesive energy per atom as a function of nearest-neighbour distance [13]) it is easy to show [10] that there exists a natural form for the inter-atomic potential,

$$\phi(r) = -\phi_0\left[1 + \delta\left(\frac{r_e}{r} - 1\right)\right]\exp\left[-\gamma\left(\frac{r_e}{r} - 1\right)\right] \tag{7}$$

and the embedding energy,

$$F(\rho) = -E_c\left(1 - \frac{\rho}{\rho_e}\ln[\rho/\rho_e]\right)\left(\frac{\rho}{\rho_e}\right)^{\alpha/\beta} + \frac{1}{2}\phi_e\sum_m s_m \exp\left[-(p_m - 1)\gamma\right] \times \left(1 + (p_m - 1)\gamma - p_m\frac{\delta}{\beta}\ln\left[\frac{\rho}{\rho_e}\right]\right)(\rho/\rho_e)^{p_m\gamma/\beta}. \tag{8}$$

Here E_c is the bulk cohesive energy and

$$\alpha = \sqrt{9B_0\Omega_0/E_c}$$

where B_0 is the equilibrium bulk modulus and Ω_0 the equilibrium atomic volume. The remaining parameters ϕ_0, δ and γ are fitted to the elastic stiffness constants and the unrelaxed monovacancy formation energy in the way originally outlined by Daw and Baskes [7].

To study a vacancy, a cubic FCC or BCC super-cell is constructed with the side length equal to a multiple of the lattice constant. One atom is removed and the lattice is allowed to relax by quenching the atom velocities each time the total kinetic energy reaches a maximum. When this energy varies by no more than 1 meV, the entire super-cell undergoes volume relaxation to produce the final zero-pressure configuration. This two-stage process is iterated until a stable minimum is obtained. In practice, only one cycle need be performed before convergence is achieved. The relaxed vacancy formation energy is then calculated via

$$E_{vf}^r = E(N-1, V) - E(N, V_0)\frac{N-1}{N} \tag{9}$$

where N is the number of atoms in the bulk super-cell. Here $E(N, V_0)$ is the total energy of the bulk super-cell at volume V_0 and $E(N-1, V)$ is the total energy of the relaxed super-cell containing the vacancy at volume V. The vacancy relaxation energy is then defined as $E^r = E^u_{vf} - E^r_{vf}$.

In an analogous way, the formation volume (the volume change due to relaxation) is given by

$$\Omega_{fv} = V - V_0 \frac{N-1}{N}. \tag{10}$$

In general the MD implementation of the EAM involves a smooth cut-off of both the inter-atomic potential and the electronic density function beyond the nearest-neighbour shell included in the fit. The form used in the present work is that detailed by Mei *et al* [10].

3. Aluminium

Using $\beta = 7.1$ [11] and $\alpha = 4.6$ [13], we fit the parameters ϕ_0, δ and γ to the experimentally known low-temperature elastic constants of aluminium [15] ($C_{11} = 0.920$, $C_{12} = 0.693$ and $C_{44} = 0.365$) and the unrelaxed vacancy formation energy E^u_{vf}. Published values for E^u_{vf} typically range between 0.6 eV and 0.9 eV [16–20]. This wide spread is thought to be primarily due to the particular choice of pseudopotential [21]. One such pseudopotential DFT study of aluminium [17] using a 32-atom super-cell obtained an unrelaxed vacancy formation energy equal to 0.78 eV. The value for E^u_{vf} implicit in the work of Mei and Davenport [11] is approximately equal to 0.785 eV. This seems a natural first choice since it is close to values used in other EAM applications to aluminium and its alloys [22, 23]. We also consider the value $E^u_{vf} = 0.86$ eV calculated by Mehl and Klein [19] who use a full-potential LAPW non-pseudopotential method and also the value $E^u_{vf} = 0.64$ eV found by Gillan [18] who uses the simple local pseudopotential given by Goodwin *et al* [24]. In both of these cases a 27-site super-cell was used.

In practice the parameters were fitted to $(C_{11} - C_{12} + 3C_{44})/5$, C_{12} and E^u_{vf} using a modified Levenberg–Marquardt algorithm together with a finite-difference Jacobian. Many good fits could be found reflecting the invariances within the EAM described by equations (3) and (4). The solution set finally chosen minimized the error in E^u_{vf}.

For $E^u_{vf} = 0.78$ eV and a third-nearest-neighbour model, the fitted values of the parameters were $\phi_0 = 0.137\,372$, $\delta = 6.849\,976$ and $\gamma = 7.220\,678$. These differ only slightly from that given by Mei and Davenport [11]. Indeed, upon comparison using the corresponding standard forms of $\phi(r)$ and $F(\rho)$, there is little noticeable difference. As a point of interest, the constant parameter β which is usually estimated via isolated Hartree–Fock wavefunctions was also regarded as a free parameter, and together with ϕ_0, δ and γ was fitted to C_{11}, C_{12}, C_{44} and E^u_{vf}. We found that equally good solutions could be obtained that were largely insensitive to β over the range 6.8 to 7.2.

The resulting inter-atomic potential drops to below 0.05% of its most negative value beyond the third-nearest-neighbour shell, thus justifying the third-nearest-neighbour approximation for aluminium. However, the contribution [25] to E^u_{vf} from each nearest-neighbour shell drops off rather more slowly beyond the first-nearest neighbour (first-shell contribution: 0.63 eV; second-shell contribution: 0.08 eV; third-shell contribution: 0.05 eV). This suggests that for greater two-digit accuracy, a model including a larger number of nearest-neighbour shells is required. We found that a fifth-nearest-neighbour model is adequate for such purposes, particularly for $E^u_{vf} = 0.86$. See figure 1 which displays the cumulative contributions to E^u_{vf} for each shell. The corresponding values of the parameters ϕ_0, δ and γ are listed in

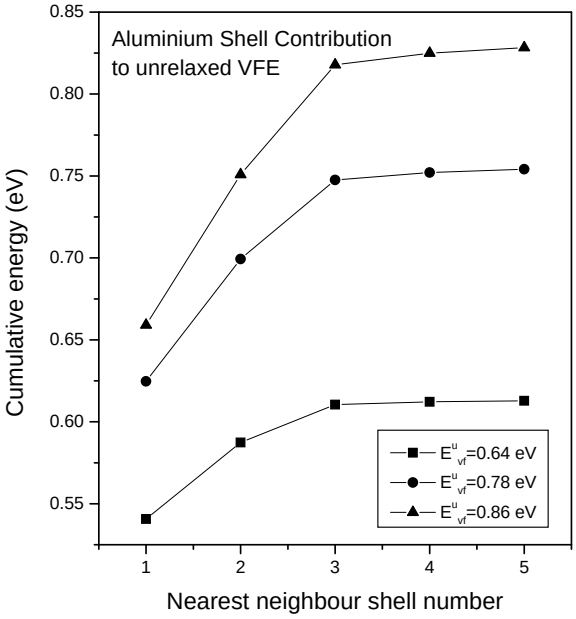

Figure 1. The cumulative contribution to the unrelaxed vacancy formation energy as a function of the shell number for aluminium. Although a third-nearest-neighbour model for aluminium is generally regarded as sufficient for MD, in the present work we use a fifth-nearest-neighbour model to achieve better two-digit accuracy in the study of vacancy relaxation.

Table 1. Fitted parameters for fifth-nearest-neighbour model for aluminium.

E^u_{vf}	ϕ_0	γ	δ
0.64	0.185989	8.020566	5.070832
0.78	0.228011	7.235296	4.292098
0.86	0.153254	6.841691	6.416339

Table 2. Calculated relaxation energies in eV for aluminium obtained using the EAM for three different unrelaxed vacancy formation energies. *Ab initio* values are also shown for comparison.

	E^u_{vf}	E^r_{vf}	E^r	Ω_{fv}
EAM	0.64	0.63	0.01	0.74
EAM	0.78	0.76	0.02	0.75
EAM	0.86	0.84	0.02	0.73
DFT (reference [18])	0.64	0.62	0.02	
DFT (reference [17])	0.78	0.71	0.07	
DFT (reference [19])	0.86	0.83	0.03	
DFT (reference [20])	0.82	0.66	0.16	0.67
Experiment		0.67†		0.62‡

† Reference [26].
‡ Reference [28].

table 1 for $E^u_{vf} = 0.64$, 0.78 and 0.86 eV. Figure 2 and figure 3 display, in standard form, the corresponding shapes of the embedding energy and the inter-atomic potential for all values of E^u_{vf}.

Table 2 lists the relaxation energies and associated formation volumes calculated using equations (9) and (10) as described in section 2. All simulations were performed using a $5 \times 5 \times 5$ super-cell with $N = 500$. For comparison, the corresponding relaxation energies obtained using *ab initio* techniques are included. We note that apart from the work of Benedek *et al* [17], our calculated relaxation energies agree closely with those obtained via *ab initio*

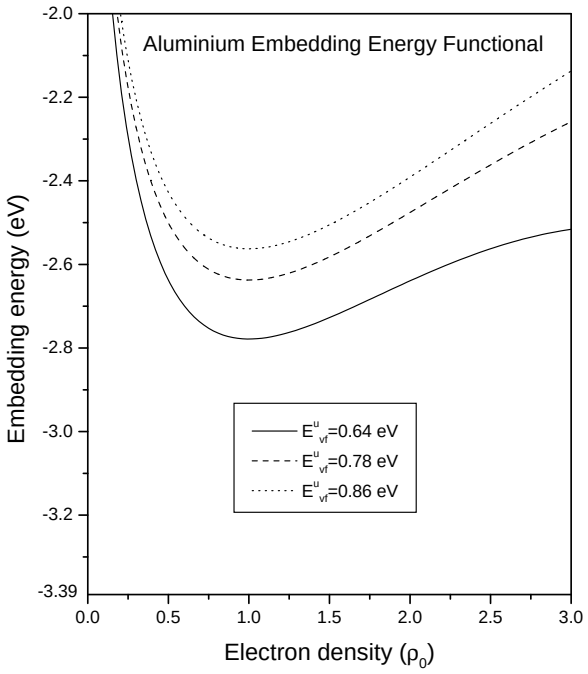

Figure 2. The embedding energy functional in standard form for aluminium with E^u_{vf} equal to 0.64, 0.78 and 0.86 eV.

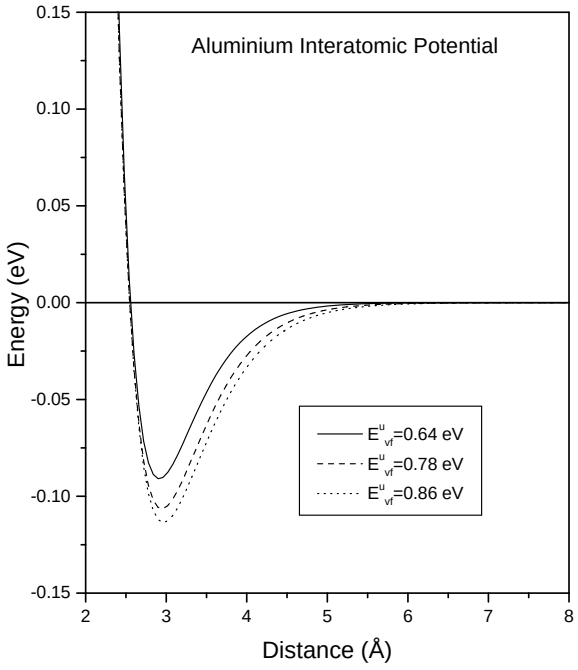

Figure 3. The inter-atomic potential in standard form for aluminium with E^u_{vf} equal to 0.64, 0.78 and 0.86 eV.

techniques. A more recent study by Chetty *et al* [20] is also included. In their work a E^u_{vf} of 0.82 eV is obtained and, via relaxation, they obtain $E^r = 0.15$ eV which is somewhat larger than the value obtained in the present work and those from the other DFT applications. The authors comment that without volume relaxation, their relaxation energy is approximately 0.08 eV, indicating a significant energy contribution due to super-cell relaxation: an effect not observed through the EAM and the other *ab initio* work [16, 17]. The recommended [26] experimental value for E^r_{vf} is 0.67 ± 0.03 eV, suggesting that for an EAM application to reproduce the correct relaxed vacancy formation energy, a value of approximately 0.7 eV should be chosen for E^u_{vf}.

Figure 4 displays the structural relaxation away from the vacancy for each nearest-neighbour cell. Again, comparison with first-nearest-neighbour DFT displacement values [17,19] reveals a close similarity with our EAM results. For the higher-order nearest-neighbour shells we see an oscillatory behaviour in which every third shell has a positive displacement. On the other hand, an early force relaxation model given by Miller and Heald [27], which assumes a simple first-nearest-neighbour pair potential, displays negative displacements for shells and thus significant deviation from our second, fifth and eighth shell. Also shown are the results of Chetty *et al* [20] for the first-, second- and third-neighbour shells. We remind the reader that all DFT relaxation calculations have been performed on super-cells containing up to 32 sites and it is currently not clear what the precise effect of such a small super-cell is on the relaxation properties of higher-order shells. This is reflected in part by our work using 32-site and 108-site super-cells (see figure 5). For the 32-site super-cell the second-, fourth- and fifth-shell displacements are completely suppressed and we find that at least an 108-site super-cell is required to begin to reproduce the relaxation profile shown in figure 4. In figure 5 we also include the results of a 108-site orbital-free *ab initio* calculation [5] and we see that

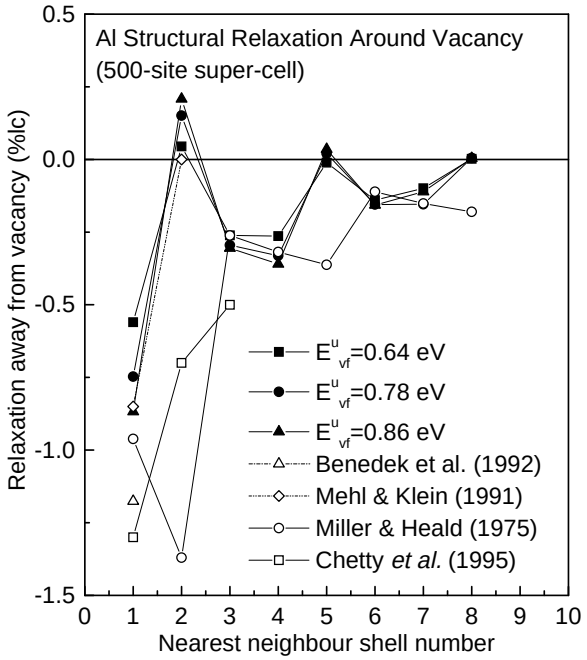

Figure 4. The structural relaxation around a vacancy in aluminium obtained using a 500-site super-cell EAM for E^u_{vf} equal to 0.64, 0.78 and 0.86 eV.

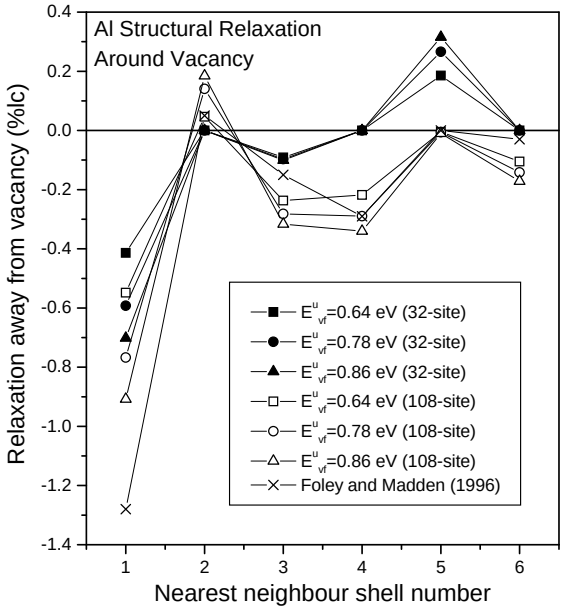

Figure 5. The structural relaxation around a vacancy in aluminium obtained using 32-site and 108-site super-cell EAMs for E^u_{vf} equal to 0.64, 0.78 and 0.86 eV. For the 32-site super-cell, interactions between the vacancy and its images clearly inhibit the relaxation process.

the EAM result is in close agreement, further substantiating the general trend of figure 4.

Like the relaxation energy, the formation volume appears insensitive to E^u_{vf}, resulting in an average value of $\Omega_{fv} = 0.75$ eV. For small lattice relaxation, the formation volume for cubic structures [27] is approximately given by

$$\Omega_{fv} = \frac{3(C_{44} - C_{12})}{C_{11} + C_{12}} + 1 \tag{11}$$

giving for aluminium, $\Omega_{fv} = 0.57$. In addition, Chetty *et al* [20] obtain a value of 0.62 ± 0.05. The EAM result compares well with these values (and experiment [28]) given the sensitivity of Ω_{fv} to chosen bulk equilibrium conditions.

4. Lithium

A similar fitting procedure to that used in the case of aluminium is applied to BCC lithium. We use a cohesive energy of 1.65 eV, $\alpha = 3.1$ (Rose *et al* [13]) and from isolated-atom Roothaan–Hartree–Fock averaged atomic wavefunctions [29], determine $\beta = 6.9$. Again, treating the latter as a free parameter does not significantly affect the form of the final inter-atomic potential and embedding energy functional. The low-temperature experimentally determined elastic stiffness coefficients for lithium [15] are $C_{11} = 0.1480$, $C_{12} = 0.125$ and $C_{44} = 0.108$. Again there are a variety of unrelaxed vacancy energies at our disposal. Frank *et al* [16] have undertaken an *ab initio* pseudopotential study of monovacancies in lithium using super-cells containing up to 54 sites, obtaining $E^u_{vf} = 0.81$ eV. On the other hand, Benedek *et al* [17] obtain, for a similar super-cell, a value of 0.66 eV. Using a first-principles pair potential calculation with a 128-site super-cell, Jacucci and Taylor [30] obtain the value 0.52 eV. We choose these values for application to the EAM model.

Application of the fitting procedure revealed that a potential consistent with a nearest-neighbour approximation could only be found if up to the ninth-nearest neighbours were included. It was only at this distance that the potential had reduced to 0.05% of its most negative value. This is not surprising despite the statement made Benedek *et al* [17] that in a MD pair potential model up to second-nearest neighbours need only be included: a justification for their use of the 54-site super-cell. The lack of p-state core electrons in lithium has the result that a component of the electron density will 'see' the full ionic potential and any realistic pseudopotential must therefore be strongly non-local. Dagens *et al* [31] have shown that the resulting inter-ionic potential is strongly oscillating and cannot be described by simple linear response theory alone, the higher-order effective potential now containing the implicit (albeit small) effects of three-body terms [32]. Indeed, a study by Duesbery *et al* [33] shows that from the perspective of Ewald lattice summation, the asymptotic Friedel oscillations can be replaced by an effective (damped) potential that for lithium extends out as far as four lattice constants.

Table 3 lists the resulting fitted parameters and figure 6 displays the cumulative contributions to the fitted unrelaxed vacancy formation energies from each shell for both values of E^u_{vf} obtained using the embedded energy functional and inter-atomic potential in their standard form. We see such contributions extending up to eight- and ninth-nearest neighbours. Figure 7

Table 3. Fitted parameters for a ninth-nearest-neighbour model for lithium.

E^u_{vf}	ϕ_0	γ	δ
0.52	0.0668747	4.885035	7.425925
0.66	0.0397088	4.141372	13.965110
0.81	0.0374230	3.622541	14.676643

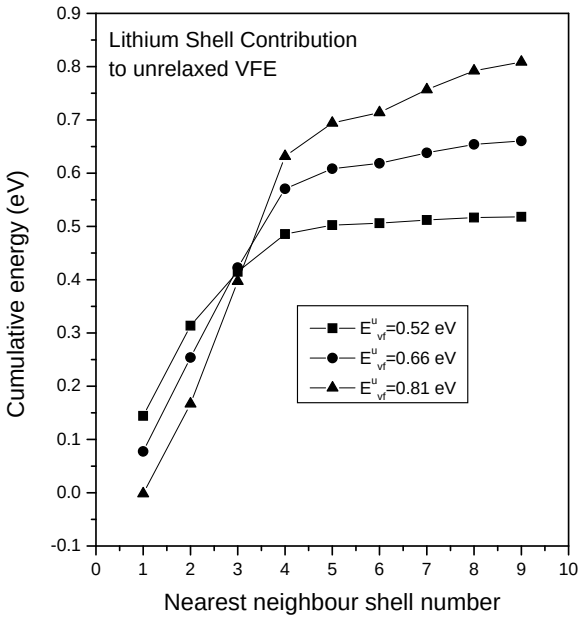

Figure 6. The cumulative contributions to the unrelaxed vacancy formation energy as functions of the shell number for a ninth-nearest-neighbour model for lithium.

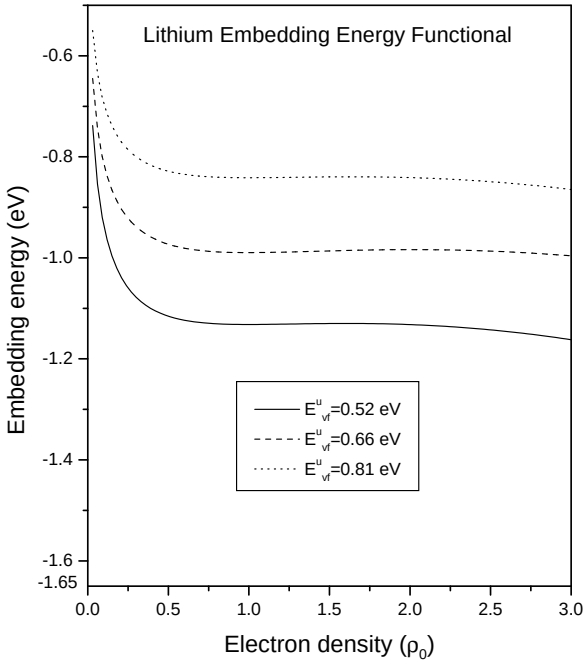

Figure 7. The embedding energy functional in standard form for lithium with E^u_{vf} equal to 0.52, 0.66 and 0.81 eV.

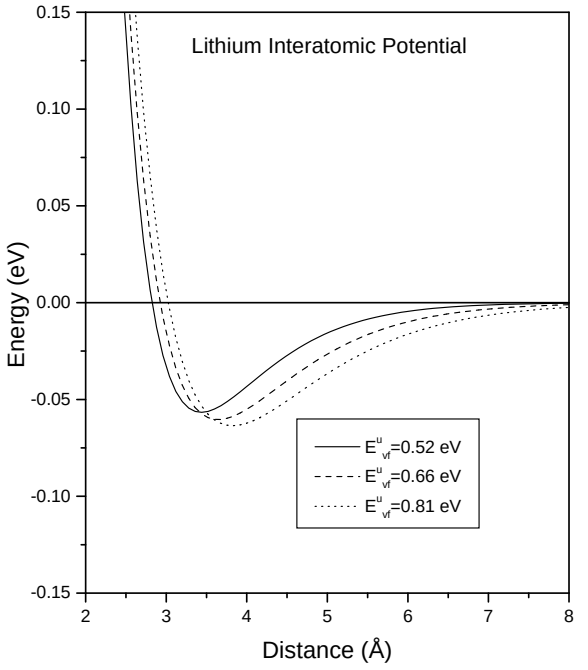

Figure 8. The inter-atomic potential in standard form for lithium with E^u_{vf} equal to 0.52, 0.66 and 0.81 eV.

and figure 8 display in standard form the shapes of the embedding energy and the inter-atomic potential for both values of E^u_{vf}, the latter clearly extending up to the ninth-nearest-neighbour distance (≈8.55 Å)

Table 4. Calculated relaxation energies in eV for lithium obtained using the EAM for three different unrelaxed vacancy formation energies. Those in parentheses employ a larger cut-off distance (see the text). *Ab initio* values are also shown for comparison.

	E^u_{vf}	E^r_{vf}	E^r	Ω_{fv}
EAM	0.52 (0.52)	0.37 (0.36)	0.15 (0.16)	0.35 (0.57)
EAM	0.66 (0.67)	0.39 (0.41)	0.27 (0.26)	−0.81 (0.69)
EAM	0.81 (0.83)	0.45 (0.36)	0.36 (0.47)	1.58 (0.52)
DFT (reference [30])	0.52–0.53	0.44–0.48	0.05–0.08	0.43
DFT (reference [17])	0.66	0.57	0.09	
DFT (reference [16])	0.81	0.54	0.27	0.49
Experiment		0.34†–0.48‡		

† Reference [34].
‡ Reference [35].

Using a 54-site super-cell with our fitted potential, it is clear that significant interaction between the vacancy and its images cannot be ruled out. Thus in the present work all simulations were performed using a $7\times7\times7$ super-cell with $N = 686$ to ensure negligible vacancy–vacancy interaction. The smooth cut-off was chosen to be just beyond the ninth-nearest neighbour. Table 4 lists the relaxation energies and corresponding formation volumes for $E^u_{vf} = 0.52$, 0.66 and 0.81 eV. Comparison with *ab initio* techniques indicates that the present EAM produces a consistently larger relaxation energy. Unlike the case for aluminium, the relaxation energy does depend strongly on the chosen value of E^u_{vf}—reducing for smaller unrelaxed vacancy formation energies. This trend is also seen in the *ab initio* calculations. Experimental values for the relaxed vacancy formation energy range from 0.34 eV [34], obtained using dilatometry, to 0.48 eV [35], obtained using the difference between the self-diffusion activation energy and the migration energy. It has been commented [17] that the latter is perhaps the more likely upon comparison with the other alkalis. Thus to construct an EAM producing the former value (0.34 eV), an unrelaxed vacancy formation energy of approximately 0.5 eV is needed and for the latter (0.48 eV), a value of approximately 0.85 eV is needed.

Inspection of the corresponding formation volumes reveals severe irregularities, suggesting that something is amiss. A look at figure 8 shows that the inter-atomic potentials for $E^u_{vf} = 0.81$ eV and 0.66 eV extend beyond the ninth-nearest-neighbour shell, indicating that we must include a greater number of nearest-neighbour shells. In the present work we simply increase the cut-off in the MD simulations to include the tenth-neighbour shell. The resulting formation energies and volumes are displayed in parentheses in table 4 and we see now that the formation volumes for different E^u_{vf} are not that dissimilar; indeed application of equation (11) to lithium gives $\Omega_{fv} = 0.56$ which compares reasonably well with the EAM results. Table 4 shows that such a modification also affects the formation energies. On increasing only the cut-off distance and not the distance to which the potential is fitted, the resulting relaxation energies in general will be slightly larger due to the additional 'bonds' entailed in the MD simulation. This effect diminishes for reducing E^u_{vf} since the potential approaches the regime in which the ninth-nearest-neighbour assumption becomes valid.

Figure 9 displays the structural relaxation away from the vacancy for each nearest-neighbour cell and displays again similar characteristics to the listed *ab initio* results, although the displacement magnitudes are consistently larger. This together with the EAM prediction

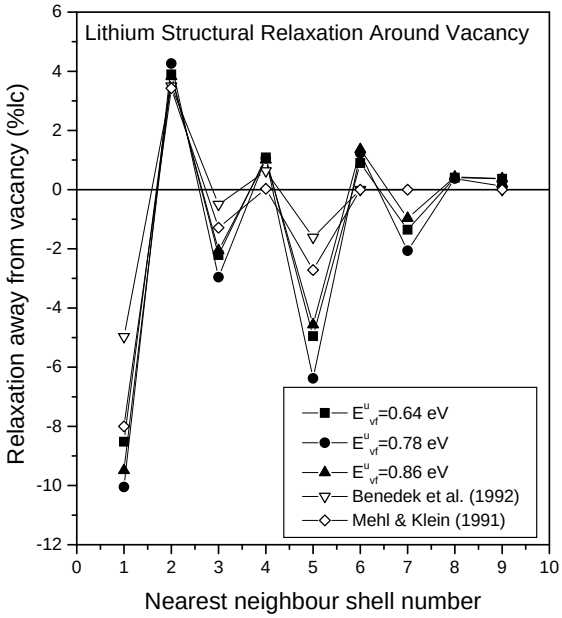

Figure 9. The structural relaxation around a vacancy in lithium obtained using a 686-site super-cell EAM for E^u_{vf} equal to 0.52, 0.66 and 0.81 eV.

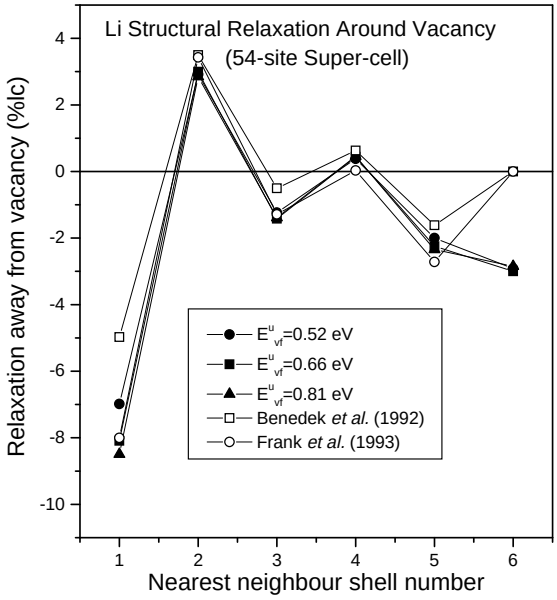

Figure 10. The structural relaxation around a vacancy in lithium obtained using a 54-site super-cell EAM for E^u_{vf} equal to 0.52, 0.66 and 0.81 eV.

of relaxation energies larger than those obtained via DFT, may simply be due to the small super-cells used in these calculations, since interactions between the vacancy and its images in general tend to inhibit the relaxation phenomena. The situation compared to that for

aluminium is somewhat better due to the larger super-cell used in the DFT calculations (54 sites corresponding to a $3 \times 3 \times 3$ super-cell). Indeed an EAM simulation using a cell of this size produced lattice displacements which agree extremely well with references [17] and [16] (see figure 10).

5. Discussion

Inspection of the embedding energy functionals for aluminium (figure 2) and lithium (figure 7) reveals that at equilibrium density, we have $F(\rho_e) \approx E_c + E^u_{vf}$ for each E^u_{vf}. Now the cohesive energy at equilibrium is defined as

$$E_c = F(\rho_e) + \frac{1}{2}\sum_m s_m \phi(r_0 p_m) \tag{12}$$

which together with $F(\rho_e) \approx E_c + E^u_{vf}$ implies

$$E^u_{vf} \approx -\frac{1}{2}\sum_m s_m \phi(r_0 p_m). \tag{13}$$

That is, the unrelaxed vacancy formation energy is defined entirely through the energy associated with breaking the inter-atomic potential 'bonds'. This is not surprising since the exact definition for E^u_{vf}:

$$E^u_{vf} = \sum_m s_m \left[F(\rho - f(r_0 p_m)) - F(\rho)\right] - \frac{1}{2}\sum_m s_m \phi(r_0 p_m) \tag{14}$$

reduces approximately to

$$E^u_{vf} \approx F'(\rho)\big|_{\rho=\rho_e} \sum_m s_m f(r_0 p_m) - \frac{1}{2}\sum_m s_m \phi(r_0 p_m) = -\frac{1}{2}\sum_m s_m \phi(r_0 p_m) \tag{15}$$

where the last equality holds only for the standard form.

For lithium, the embedding energy is almost a constant for a wide range of local densities, indicating that local variations in density do not significantly affect the electronic contribution to the cohesive energy. This is no doubt due to the extended nature of its inter-atomic potential. Indeed, for lithium we have $C_{12} - C_{44} = 0.017$ which almost satisfies the first Cauchy relation for cubic structures: $C_{12} - C_{44} = 0$; that is, that the primary bonding is due to central-force interactions. This is further substantiated by $C_{12} - C_{44}$ formally being defined as the curvature of the embedding energy with respect to density variations [7]. Figure 7 clearly reflects this. On the other hand, for aluminium, figure 2 displays a clear positive curvature which simply reflects the fact that for this material $C_{12} - C_{44} = 0.328$. That is, a significant component of the cohesive energy is electronic.

Thus application of the EAM to lithium demonstrates that for MD configurations in which the local density does not change drastically, an equivalent pair potential model plus a constant electronic term will suffice to reproduce the correct cohesive energy. We emphasize that this is for reasons generally different from those operative for simple closed-shell systems (for example helium), where the embedding energy is entirely a linear function of density. In the case of lithium, the large inter-atomic potential is far more dominant than the dynamical response of the electronic contribution to the cohesive energy, whereas for closed-shell systems there is little or no electronic contribution.

Due to the negligible curvature of the embedding functional of lithium, the elastic stiffness constants will depend primarily on the curvature of the inter-atomic potential [36]. With equation (13) in mind and the relatively small experimental values of C_{11}, C_{12} and C_{44} for

lithium, this suggests that the fitted inter-atomic potential as a function of increasing unrelaxed vacancy formation energy should tend outward to accommodate larger values of E^u_{vf}. Figure 8 displays such a trend. Typically, such an effect tends not to alter greatly the relative forces between particles, thus explaining the insensitivity of structural relaxation as a function of E^u_{vf} (figure 9). On the other hand, relative energies do change, as indicated in table 4, as a result of the relaxation energies for lithium depending on E^u_{vf}. This is also reflected in figure 6 where the distribution of contributions to the unrelaxed vacancy formation energy from each neighbour shell changes for increasing values of E^u_{vf}.

For aluminium both the structural relaxation around the vacancy and the relaxation energy are an order of magnitude smaller than for lithium. In part, this is due to the shorter-range inter-atomic potential and the greater role played by the density term. Furthermore, the curvature of the aluminium embedding energy around the equilibrium point (figure 6) is insensitive to E^u_{vf}, leading to a corresponding insensitivity of the relaxation energy. Together, these trends justify the use of simply the experimental vacancy formation energy as an empirical input to EAM applications for aluminium.

6. Concluding remarks

The primary advantage of the EAM is that unlike in *ab initio* methods there is little restriction on the size of the super-cell. Where, in the latter, relaxation calculations have been primarily performed using super-cells with side lengths of two lattice constants for aluminium and three for lithium, we have demonstrated that at least a $3 \times 3 \times 3$ super-cell is required to begin to approach the converged result. To obtain converged results for aluminium a 500-site $5 \times 5 \times 5$ super-cell and for lithium a 686-site $7 \times 7 \times 7$ super-cell have been employed—a regime for which orbital DFT is not yet feasible. For aluminium however, orbital-free DFT has been applied to super-cells containing in the region of 108 and 256 sites [5, 37] demonstrating relaxation properties similar to those predicted by the EAM (although the formation and relaxation energies differ significantly from those obtained from our work and orbital-based DFT). For this material a good local potential description exists; however, as already discussed, for lithium such local potentials do not exist and there is considerable interest in extending the orbital-free framework to non-local potentials (see the discussion in reference [5]).

The disadvantage of the EAM is that it requires the unrelaxed vacancy formation energy (together with the elastic stiffness constants) as input to complete the semi-empirical formalism. In the present work we have demonstrated the relative insensitivity of this parameter to the lattice relaxation dynamics of pure materials. For aluminium, the relaxation energy also appears to be insensitive; however, for lithium this is not quite the case. Furthermore, for lithium, unlike aluminium, the published experimental values for E^r_{vf} cover a broad range. The choice of which value to use for lithium may significantly affect the dynamics and kinetics of an EAM application to the aluminium–lithium system. In future work we will investigate this possible dependence by studying the diffusion properties of lithium in aluminium in the presence of vacancies.

Acknowledgment

PMD acknowledges the financial support of the Norwegian Research Council (Grant No 116559/431)

References

[1] Car R and Parrinello M 1985 *Phys. Rev. Lett.* **55** 2471
[2] Remler D K and Madden P A 1990 *Mol. Phys.* **70** 921
[3] Wang L-W and Teater M P 1992 *Phys. Rev.* B **45** 13 196
[4] Smargiassi E and Madden P A 1994 *Phys. Rev.* B **49** 5220
[5] Foley M and Madden P A 1996 *Phys. Rev.* B **53** 10 589
[6] Daw M S and Baskes M I 1983 *Phys. Rev. Lett.* **50** 1285
[7] Daw M S and Baskes M I 1984 *Phys. Rev.* B **29** 6443
[8] Zhou S J, Preston D L, Lomdahl P S and Beazley D M 1998 *Science* **279** 1525
[9] Johnson R A 1989 *Phys. Rev.* B **39** 12 554
[10] Mei J, Davenport J W and Fernando G W 1991 *Phys. Rev.* B **43** 4653
[11] Mei J and Davenport J W 1992 *Phys. Rev.* B **46** 21
[12] Johnson R A 1988 *Phys. Rev.* B **37** 3924
[13] Rose J H, Smith J R, Guinea F and Ferrante J 1984 *Phys. Rev.* B **29** 2963
[14] Chen Nan-xian, Chen Zhao-doe and Wei Yu-chuan 1997 *Phys. Rev.* E **55** 1
[15] Simmons G and Wang H 1971 *Single Crystal Elastic Constants and Calculated Aggregate Properties: a Handbook* (Cambridge, MA: MIT Press)
[16] Frank W, Breier U, Elsässer C and Fähnle M 1993 *Phys. Rev.* B **48** 7676
[17] Benedek R, Yang L H, Woodward C and Min B I 1992 *Phys. Rev.* B **45** 2607
[18] Gillan M J 1989 *J. Phys.: Condens. Matter* **1** 689
[19] Mehl M J and Klein B M 1991 *Physica* B **172** 211
[20] Chetty N, Weinert W, Rahman T S and Davenport J W 1995 *Phys. Rev.* B **52** 6313
[21] Jansen R W and Klein B M 1989 *J. Phys.: Condens. Matter* **1** 8359
[22] Voter A F and Chen S P 1990 *Mater. Res. Soc. Symp. Proc.* **82** 175
[23] Voter A F 1994 *Principles (Intermetallic Compounds vol 1)* ed J H Westbrook and R L Fleischer (New York: Wiley) p 77
[24] Goodwin L, Needs R J and Heine V 1990 *J. Phys.: Condens. Matter* **2** 351
[25] By this we mean the combined (negative) energy contribution associated with the breaking of bonds and changing of electronic density on the formation of a monovacancy.
[26] Ehrhart P, Jung P, Schulta H and Ullmaier H 1990 Atomic defects in metals *Landolt–Börnstein New Series* Group III, vol 25, ed H Ullmaier (Berlin: Springer)
[27] Miller K M and Heald P T 1975 *Phys. Status Solidi* b **67** 569
[28] Hatch J E 1984 *Aluminium: Properties and Physical Metallurgy* (Metals Park, OH: American Society of Metals)
[29] Clementi E and Roetti C 1974 *At. Data Nucl. Data Tables* **14** 177
[30] Jacucci G and Taylor R 1979 *J. Phys. F: Metal Phys.* **9** 1489
[31] Dagens L, Rasolt M and Taylor R 1975 *Phys. Rev.* B **11** 2726
[32] Harrison W A 1980 *Electron Structure and the Properties of Solids* (New York: Freeman) section 17-b
[33] Duesbery M S, Jacucci G and Taylor R 1979 *J. Phys. F: Met. Phys.* **9** 413
[34] Feder R 1970 *Phys. Rev.* B **4** 828
[35] Schultz H 1991 *Mater. Sci. Eng.* **4** 1
[36] See equations (8) to (10c) in reference [7].
[37] Jessen B J, Foley M and Madden P A 1997 *Phys. Rev.* B **55** 4941